Electronic Supplementary Information

Nonaqueous potassium-ion hybrid capacitor enabled by two-dimensional diffusion pathways of dipotassium terephthalate

Yuwen Luo,‡[ab] Luojia Liu,‡[b] Kaixiang Lei,[b] Jifu Shi,*[c] Gang Xu,[a] Fujun Li,*[b] and Jun Chen[b]

[a] Guangzhou Institute of Energy Conversion, Key Laboratory of Renewable Energy, Guangdong Provincial Key Laboratory of New and Renewable Energy Research and Development, Chinese Academy of Sciences, Guangzhou 510640, China
University of Chinese Academy of Sciences, Beijing 100049, China

[b] Key Laboratory of Advanced Energy Materials Chemistry (Ministry of Education) College of Chemistry, Nankai University, Tianjin 300071, China
E-mail: fujunli@nankai.edu.cn

[c] Siyuan Laboratory, Department of Physics, Jinan University, Guangzhou 510632, China
E-mail: shijifu2017@126.com

Experimental Section

Materials and Synthesis. K_2TP was synthesized via acid base neutralization reaction between terephthalic acid (TPA) and KOH in aqueous solution. Firstly, 2.0 g of KOH was dissolved in 30 mL of deionized water, into which 1.8 g of TPA was added at 60 °C. The resultant product was precipitated by adding absolute ethanol at 90 °C. After refluxing at 90 °C for 10 h, the as-prepared product was centrifuged and washed three times with ethanol. Finally, the product was dried in vacuum at 100 °C for 10 h. Activated carbon (AC) of YEC-8B was purchased from Fuzhou Yihuan Carbon Co., Ltd. (China) without treatment before use.

Characterization. K_2TP and its corresponding electrodes at different states during cycling were characterized by field-emission scanning electron microscopy (FE-SEM, JEOL JSM-7500F), Fourier transform infrared spectroscopy (FTIR, BIORAD FTS 6000), powder X-ray diffraction (XRD, Rigaku X-2500 diffractometer) using Cu Kα radiation, Raman spectroscopy (Thermo-Fisher-Scientific, excitation wavelength of 532 nm), and transmission electron microscopy (TEM, JEOL JEM-2800). AC was characterized by FE-SEM, TEM, and low-temperature nitrogen sorption experiment by a volumetric adsorption apparatus of BELSORP-mini II (BEL JAPAN, INC.).

Electrochemical measurements. CR2032 coin cells were applied to investigate electrochemical performances of K_2TP electrode, AC electrode, and KIHC. All the coin cells were assembled in an Ar-filled glove box, where contents of O_2 and H_2O are both below 1.0 ppm. Before preparing the electrode, K_2TP was ball milled with Super P carbon black (SP) with a mass ratio of 6:3 in a planetary mill at 350 rpm for 2 h. The K_2TP electrode was prepared by casting the slurry onto a copper foil, where 90% of K_2TP/SP and 10% of poly(vinylidene fluoride) (PVDF) in N-methyl-2-pyrrolidone (NMP), and vacuum-dried at 110 °C for 10 h. The mass loading of active material in electrodes with a diameter of 12 mm

is 1.2-1.5 mg cm^{-2}. For Raman tests, the K_2TP electrode was composed of K_2TP, copper powder and PVDF with a mass ratio of 5:4:1. The AC electrode was fabricated by throughly blending AC, SP and polytetrafluoroethylene (PTFE*)* with a weight ratio of 8:1:1. Then, the paste was pressed onto a stainless steel mesh of 12 mm in size under 5.0 MPa and dried in vacuum at 100 °C for 10 h. The mass loading of active material in AC electrode is 4.8-6.0 mg cm^{-2}. In half batteries, potassium metal was used as negative electrode. Before assembling full batteries of KIHC, both K_2TP anode and AC cathode underwent an activation process to remove the irreversible capacity by performing three cycles in half batteries at 100 mA g^{-1}. Glassy-fiber filter was employed as separator. The electrolyte was 1.5 M of KPF_6 in 1,2-dimethoxyethane (DME). 12.0 μL of the electrolyte was applied in each coin cell. Galvanostatic charge/discharge tests were performed on Land CT2001A battery instrument. Cyclic voltammetry (CV) and electrochemical impedance spectroscopy (EIS) were tested on an electrochemical workstation of Solartron 1470E. All of electrochemical measurements were carried out at room temperature. The electrodes were taken out from the cycled cells in the glovebox and washed by DME to remove the residual electrolyte before characterization.

Computational Method. The dispersion-corrected density functional theory (DFT-D2) calculations of potassium terephthalate (K_4TP) were performed using Vienna ab-initio simulation package (VASP) with the generalized gradient approximation (GGA) and the Perdew-Burke-Eznerhof (PBE) functional (GGA-PBE) to describe the exchange-correlation energy of electrons.[1-5] The projector-augmented wave method (PAW) was used to treat the interaction between the atomic cores and electrons.[6,7] For the geometry optimization, the reciprocal space was covered by a 4×8×4 Monkhorst-Pack k-point grid with Γ point and a cutoff of 450 eV was used for K_4TP primitive cell (~11 Å×4 Å×12 Å).[8] Atomic positions and cell vectors were fully optimized until all force components were less than 0.02 eV $Å^{-1}$. The ab-initio molecular dynamic (AIMD) simulation was performed to roughly examine the possible K^+ diffusion pathways for 10 ps with 1 fs time steps. To keep the computational cost

at a reasonable level, we used a 2×4×2 Monkhorst-Pack k-point mesh with Γ point sampling and a 400 eV cutoff in MD calculations.[8] The same conditions were used in CI-NEB calculations and all atomic positions and cell vectors were optimized until all force components were less than 0.04 eV $Å^{-1}$.[9,10] The structural optimization and Raman spectrum simulation of K_2TP and K_4TP were carried out using Gaussian 16 software package[11] with b3lyp/6-31+g(d,p)[12] level of theory.

Table S1. Refined structural parameters of K_2TP by the Rietveld method.

atom	site	occ.	x	y	z
K1	4e	1	0.613041	0.204976	0.163486
O1	4e	1	0.350194	0.166551	0.165236
O2	4e	1	0.325817	0.312560	-0.033098
C1	4e	1	0.133960	0.395461	0.020762
C2	4e	1	0.087819	0.355026	0.124919
C6	4e	1	0.054112	0.570759	-0.090440
C7	4e	1	0.293040	0.278809	0.055209
H2A	4e	1	0.106948	-0.260348	0.283125
H6A	4e	1	0.096918	0.311481	-0.159853

[α] Monoclinic, space group P21/c, a=10.552 Å, b=3.935 Å, c=11.520 Å, β=113.08°, and V=440.05 Å^3 (χ^2=1.347, R_{wp}=14.19% and R_p=10.25%).

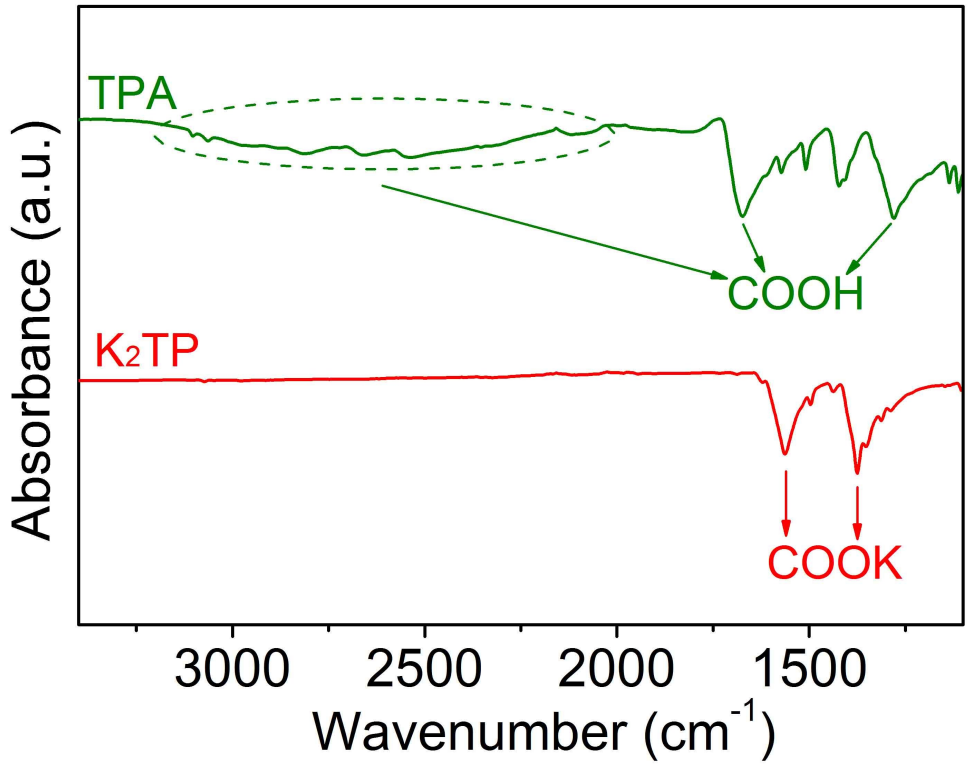

Fig. S1 FTIR spectra of TPA and K_2TP. After reaction of TPA with KOH, emergence of the characteristic peaks for –COOK (1564 and 1375 cm^{-1}) and disappearance of the peaks for –COOH (3200-2000, 1676 and 1420 cm^{-1}) confirm formation of K_2TP.

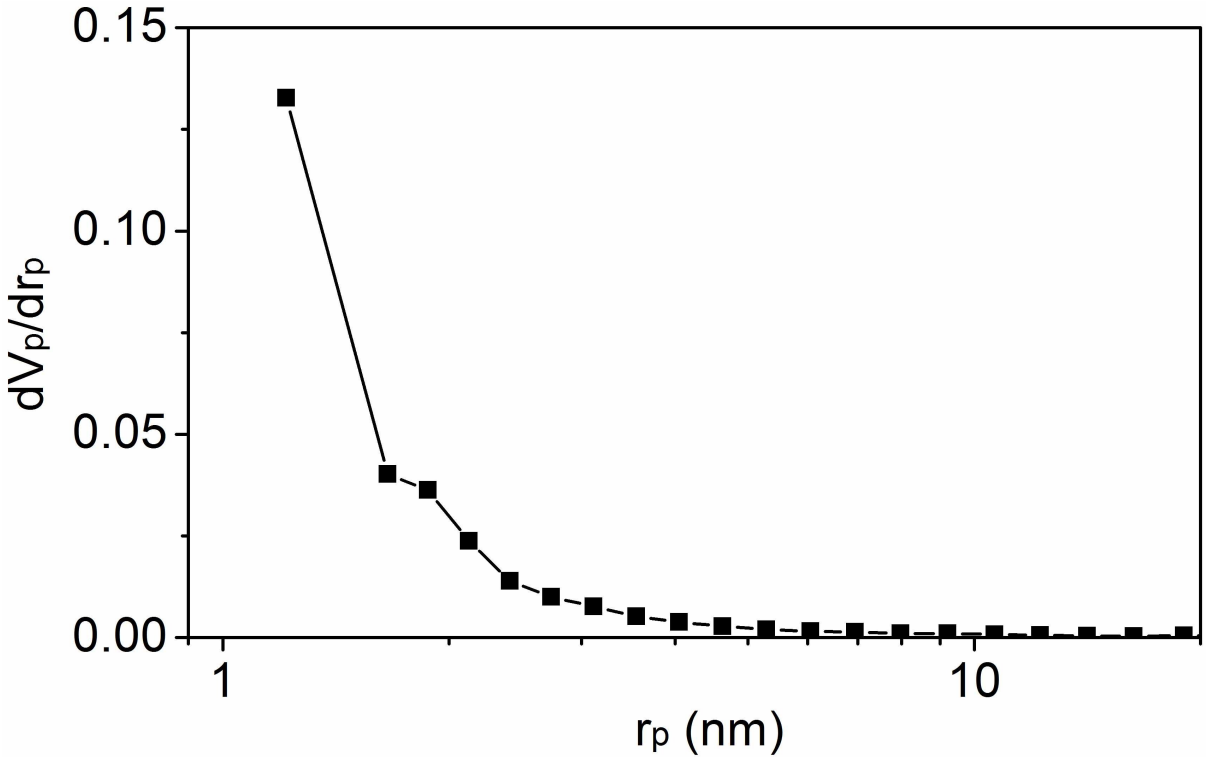

Fig. S2 Pore size distribution of AC.

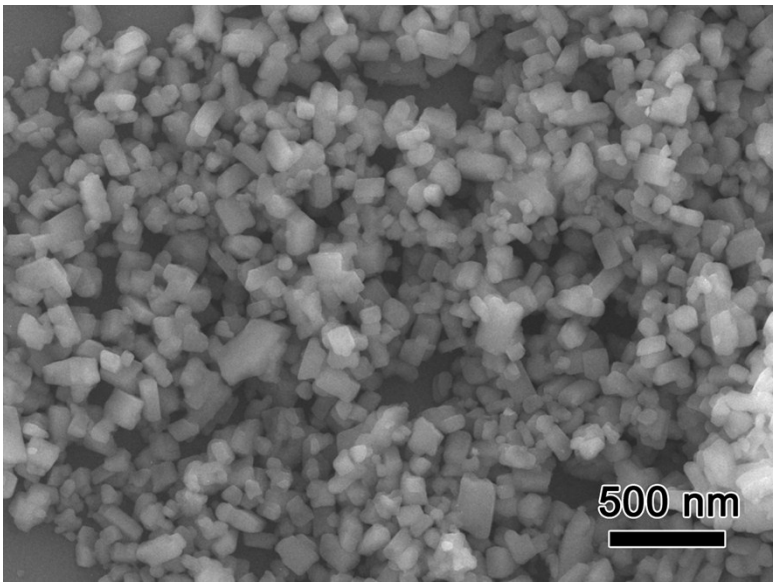

Fig. S3 SEM image of ball-milled K_2TP.

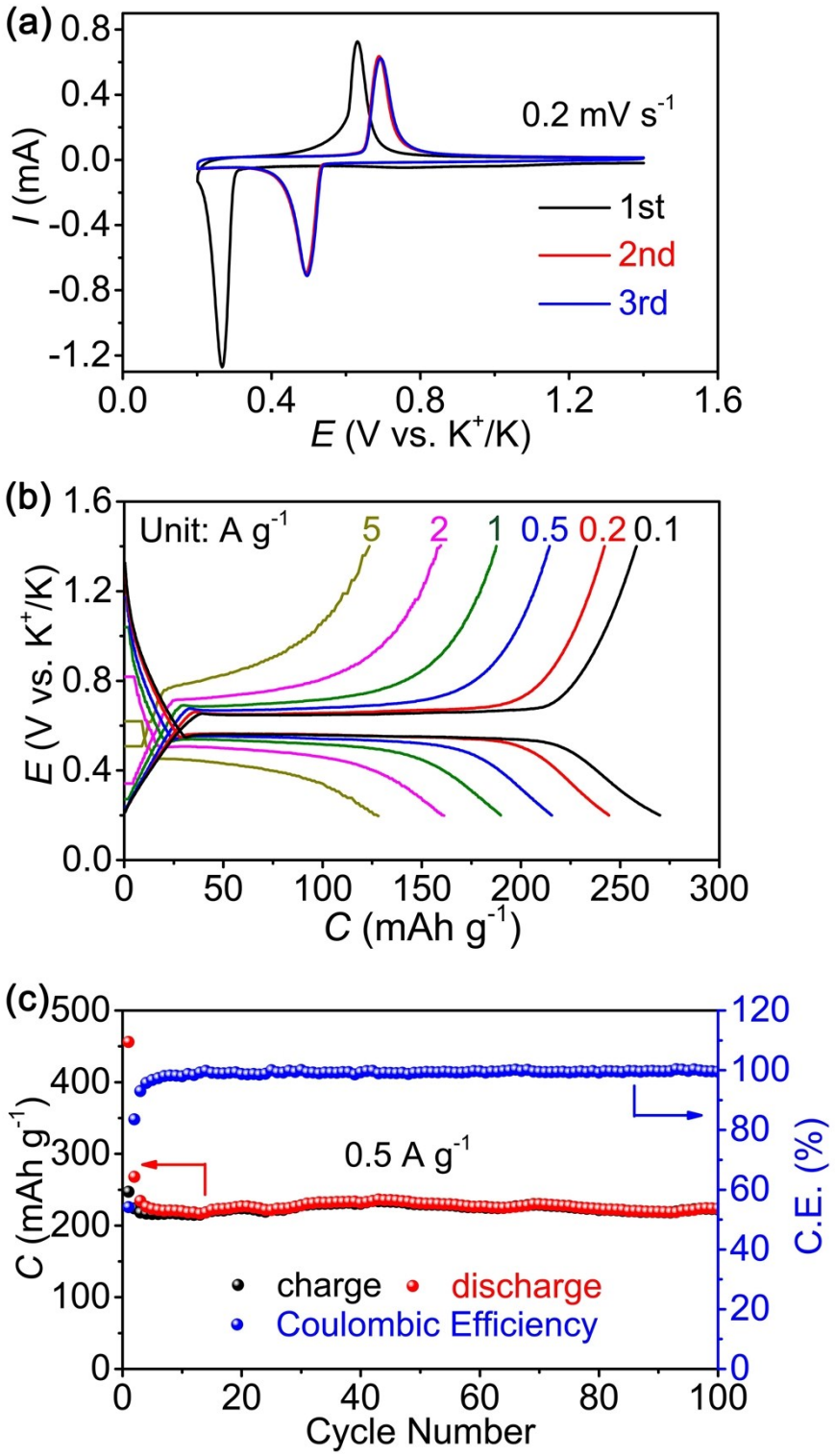

Fig. S4 Electrochemical performance of K//K_2TP half batteries in the voltage range of 0.2–1.4 V. (a) CV curves at 0.2 mV s^{-1}; (b) Typical discharge and charge curves at different current rates; (c) Cycle stability at 500 mA g^{-1}.

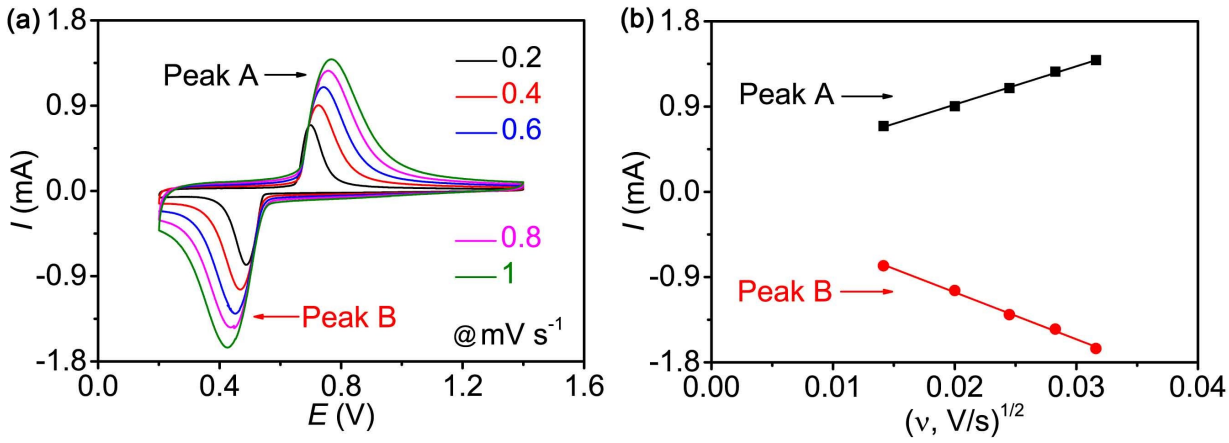

Fig. S5 (a) CV curves of K//K_2TP half battery at different scan rates; and (b) the corresponding relationship between the peak current (i_p) and the square root of scan rate ($v^{1/2}$).

Randles-Sevcik equation:

$$i_p = (2.69\times10^5)n^{3/2}AD_{K^+}^{1/2}C_{K^+}v^{1/2} \quad \text{.....(Equation S1)}$$

Where i_p represents peak current (A), n stands for charge-transfer number, A is contact area between electrolyte and electrode, D_{K+} is diffusion coefficient of K^+ (cm^2 s^{-1}), C_{K^+} is concentration of K^+ in the K_2TP electrode material, and v is scan rate (V s^{-1}).

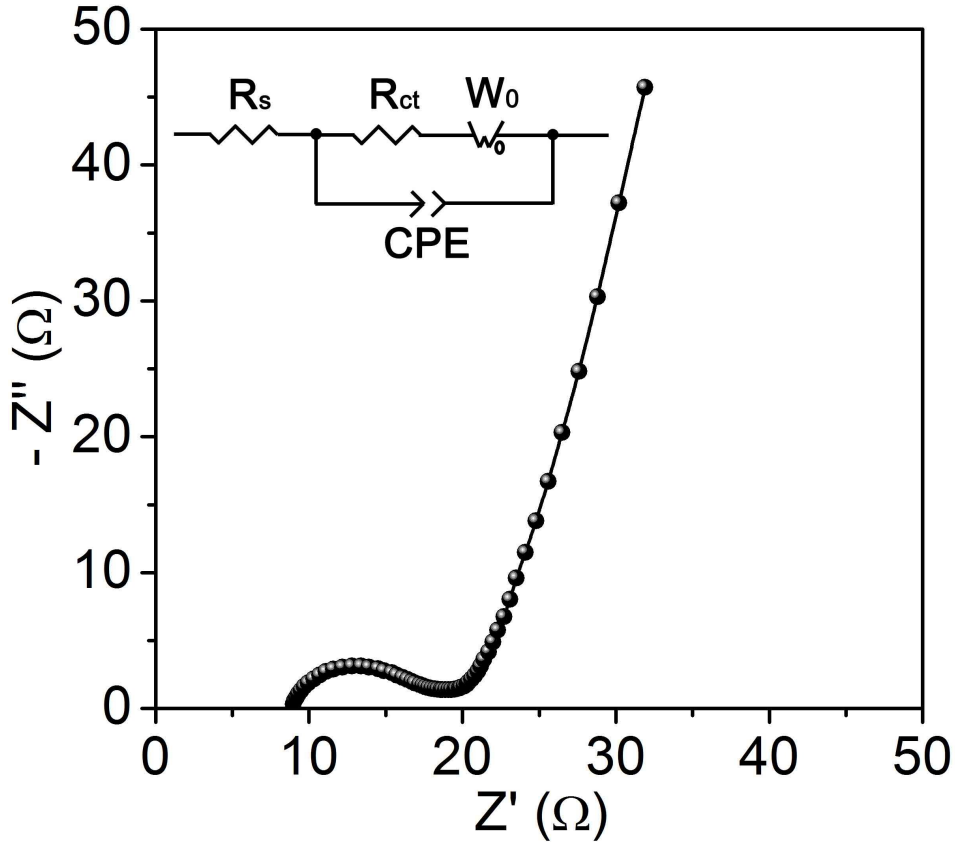

Fig. S6 EIS plots of K//K_2TP half battery at open-circuit voltage. The charge transfer resistence of K_2TP is estimated to 9.1Ω by the fitted result of the equivalent circuit (inset).

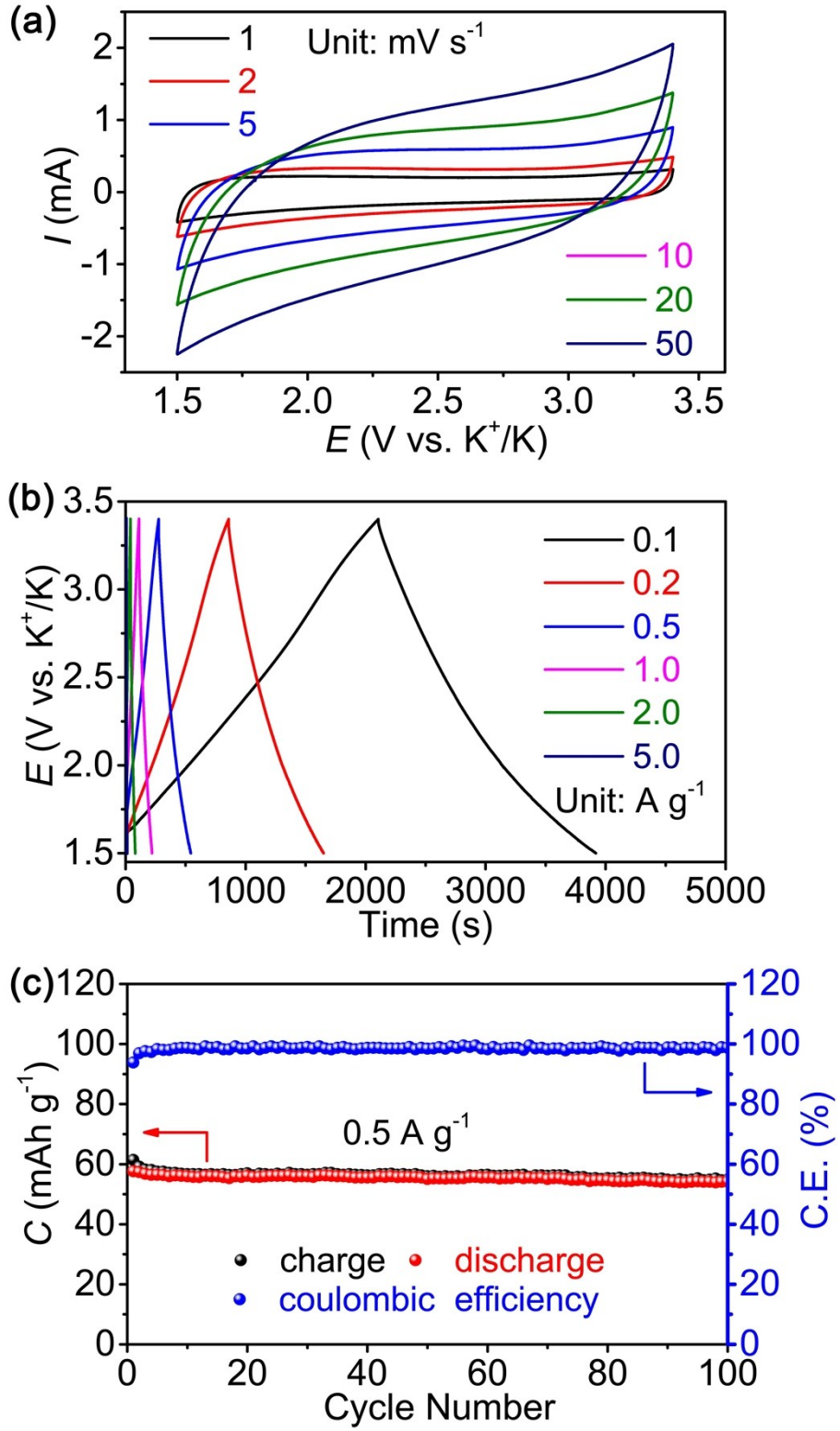

Fig. S7 Electrochemical performance of K//AC half batteries in the voltage range of 1.5-3.4 V. (a) CV curves at different scan rates; (b) Galvanostatic charge/discharge voltage profiles at different current densities; (c) Cycle stability at 500 mA g^{-1}.

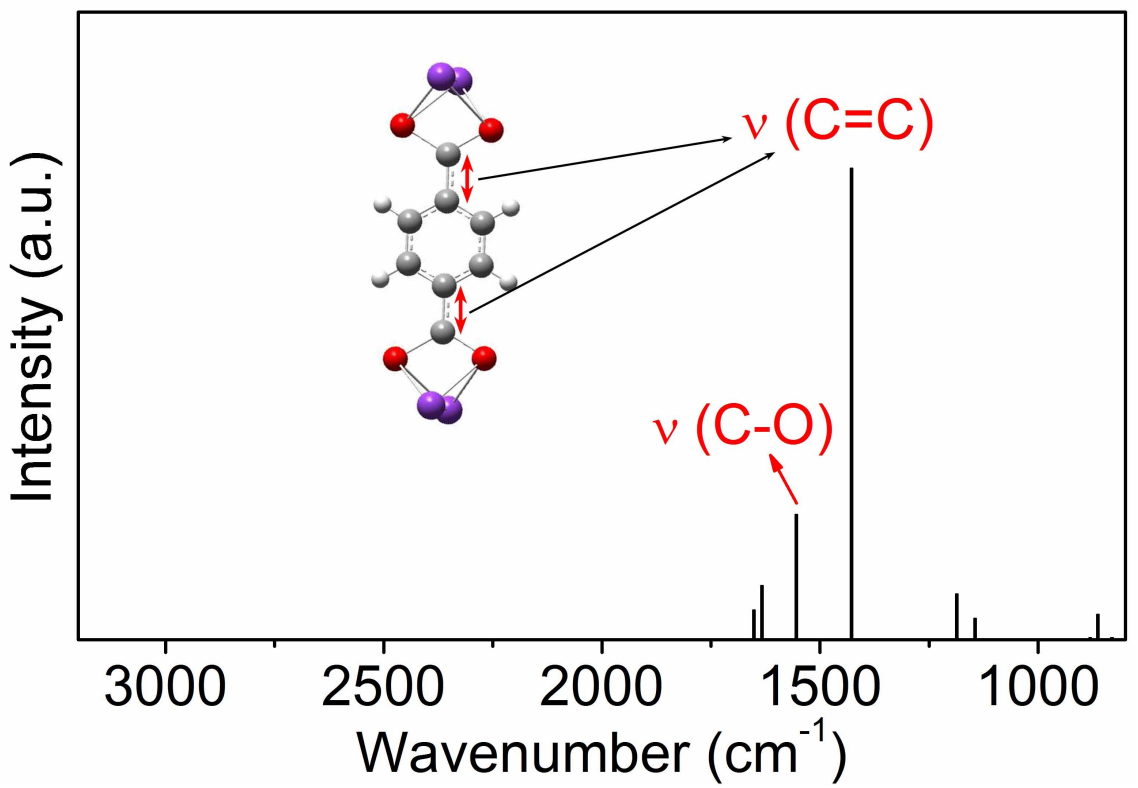

Fig. S8 Simulated Raman spectrum of the optimized molecule of K_4TP.

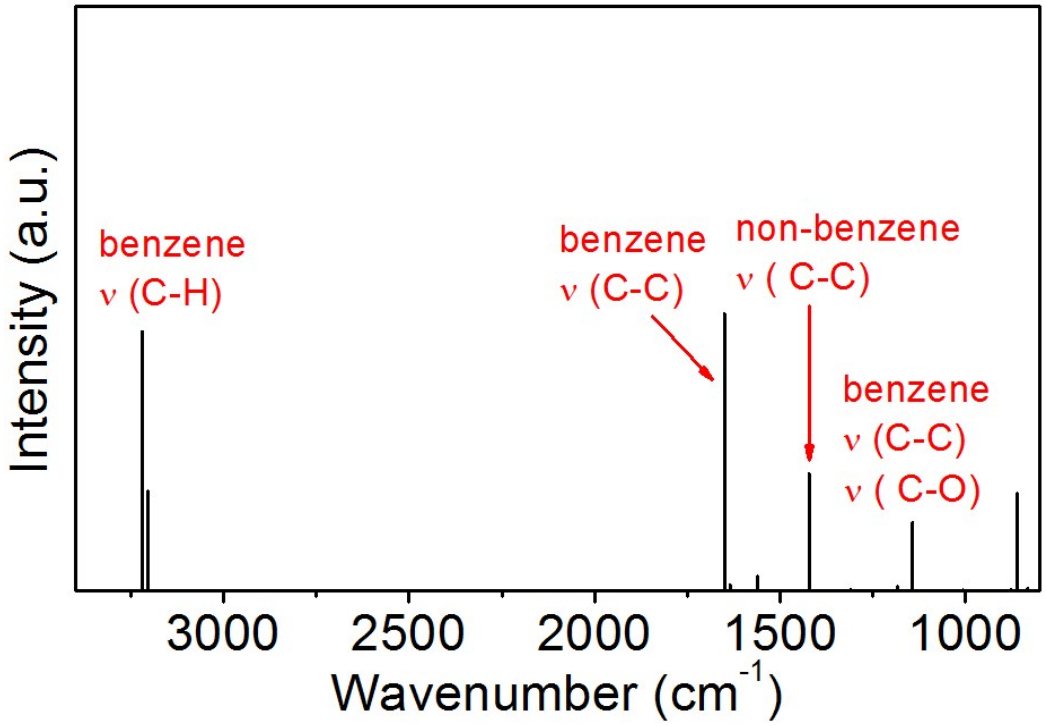

Fig. S9 Simulated Raman spectrum of K_2TP.

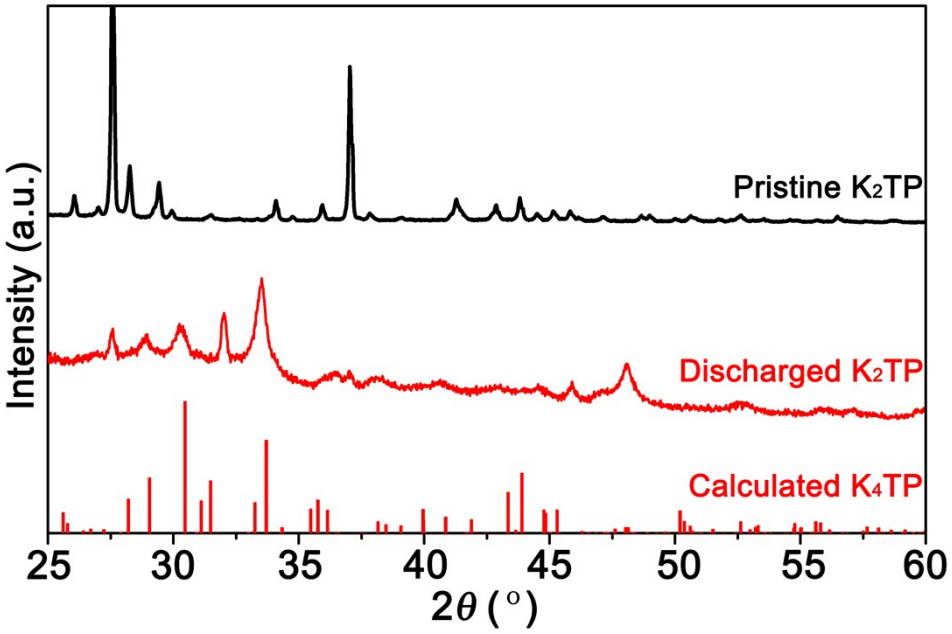

Fig. S10 XRD patterns of the pristine and discharged K_2TP (namely, K_4TP) and the calculated K_4TP.

Table S2. Cell parameters of K_4TP.

a	**10.842 Å**
b	**4.122 Å**
c	**11.549 Å**
α	**90.00°**
β	**111.12°**
γ	**90.01°**
V	**481.40 $Å^3$**

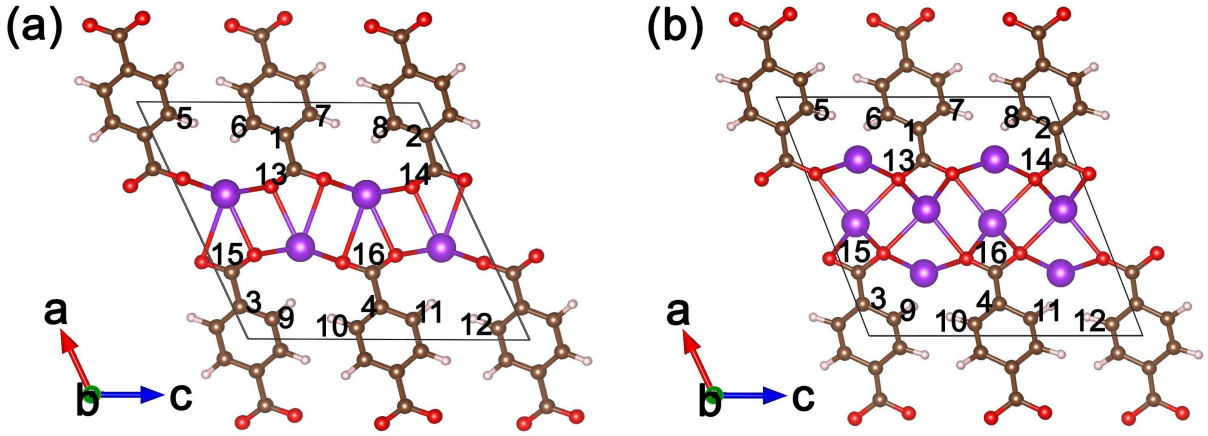

Fig. S11 Positions of carbon atoms of a) K_2TP and b) K_4TP for Bader charge calculation.

Table S3. Bader charge change in K_2TP and K_4TP.

		K_2TP	K_4TP	
Position	**ATOM**	**CHARGE**	**CHARGE**	**Difference**
1	**C**	**4.0596**	**3.9624**	**-0.0972**
2	**C**	**4.0596**	**3.9675**	**-0.0921**
3	**C**	**4.0596**	**4.004**	**-0.0556**
4	**C**	**4.0596**	**4.005**	**-0.0546**
5	**C**	**4.0526**	**4.085**	**0.0324**
6	**C**	**4.0254**	**4.0581**	**0.0327**
7	**C**	**4.0254**	**4.0617**	**0.0363**
8	**C**	**4.0254**	**4.0662**	**0.0408**
9	**C**	**4.0254**	**4.0781**	**0.0527**
10	**C**	**4.0526**	**4.113**	**0.0604**
11	**C**	**4.0526**	**4.1267**	**0.0741**
12	**C**	**4.0526**	**4.1339**	**0.0813**
13	**C**	**2.4078**	**2.8783**	**0.4705**
14	**C**	**2.4078**	**2.8803**	**0.4725**
15	**C**	**2.4078**	**2.9315**	**0.5237**
16	**C**	**2.4078**	**2.9346**	**0.5268**
	H	0.9382	0.9925	0.0543
	H	0.9382	0.9937	0.0555
	H	0.9382	1.0112	0.073
	H	0.9382	1.0129	0.0747
	H	0.9205	1.0123	0.0918
	H	0.9205	1.0156	0.0951
	H	0.9205	1.0247	0.1042
	H	0.9205	1.0512	0.1307
	O	7.2322	7.2597	0.0275
	O	7.2322	7.2603	0.0281
	O	7.2322	7.268	0.0358
	O	7.2322	7.2682	0.036
	O	7.2294	7.2713	0.0419
	O	7.2294	7.2716	0.0422
	O	7.2294	7.2717	0.0423
	O	7.2294	7.2732	0.0438

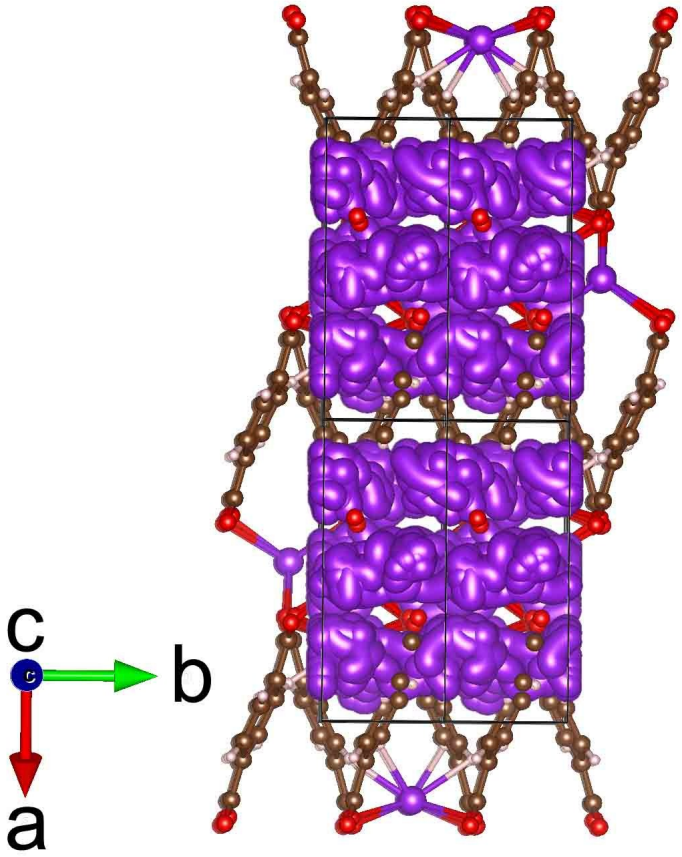

Fig. S12 Calculated trajectories of K^+ in K_4TP along *c* axis.

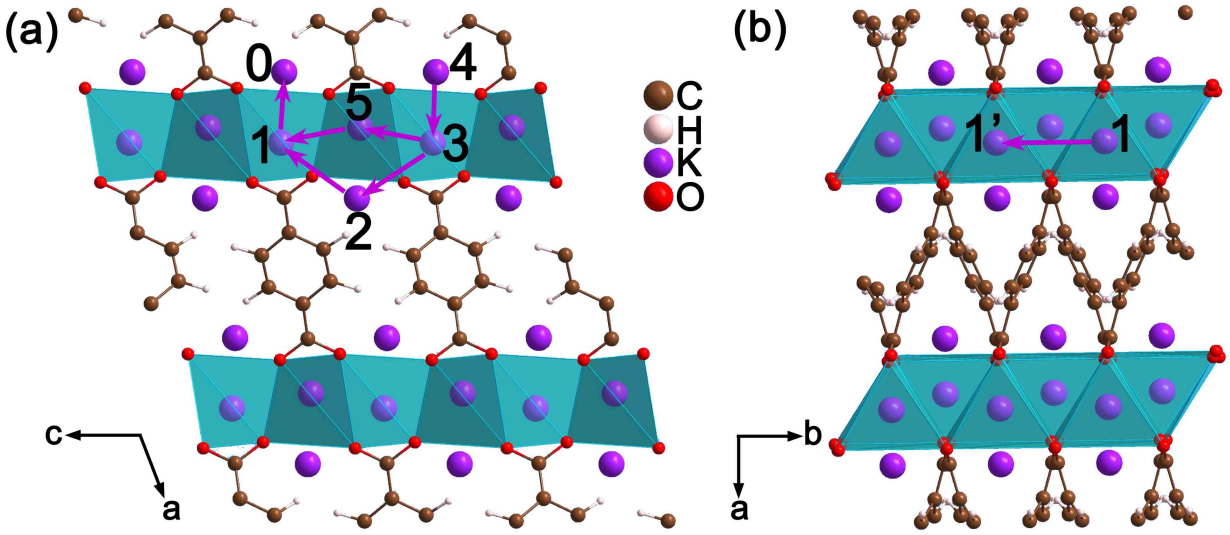

Fig. S13 Designed K^+ diffusion paths in K_4TP are shown in different directions. a) Path A (4→3→5→1→0) and path B (4→3→2→1→0); b) Path C (1→1').

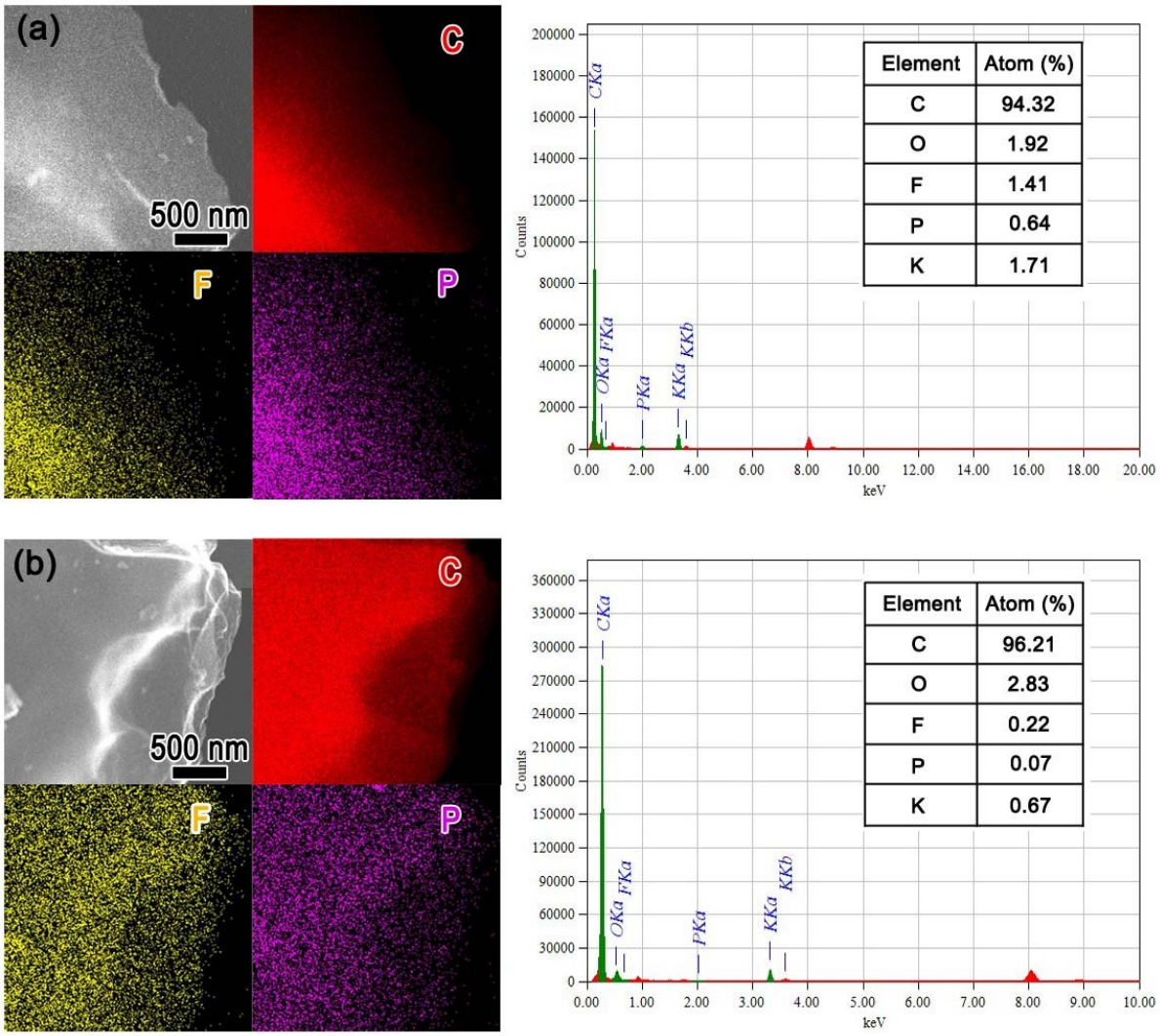

Fig. S14 TEM images of AC electrodes at different states in KIHC: (a) fully charged state and (b) fully discharged state.

References

1 S. Grimme, *J. Comput. Chem.* 2006, **27**, 1787.

2 J. P. Perdew, K. Burke and M. Ernzerhof, *Phys. Rev. Lett.* 1996, **77**, 3865.

3 G. Kresse and J. Hafner, *Phys. Rev. B* 1993, **48**, 13115.

4 G. Kresse and J. Furthmüller, *Phys. Rev. B* 1996, **54**, 11169.

5 G. Kresse and J. Furthmüller, *J. Comput. Mater. Sci.* 1996, **6**, 15.

6 P. E. Blöchl, *Phys. Rev. B* 1994, **50**, 17953.

7 G. Kresse and D. Joubert, *Phys. Rev. B* 1999, **59**, 1758.

8 H. J. Monkhorst and J. D. Pack, *Phys. Rev. B* 1976, **13**, 5188.

9 G. Henkelman, B. P. Uberuaga and H. Jónsson, *J. Chem. Phys.* 2000, **113**, 9901.

10 G. Henkelman and H. Jónsson, *J. Chem. Phys.* 2000, **113**, 9978.

11 M. J. Frisch, G. W. Trucks, H. B. Schlegel, G. E. Scuseria, M. A. Robb, J. R. Cheeseman, G. Scalmani, V. Barone, B. Mennucci, G. A. Petersson, et al. Gaussian 09; Gaussian Inc.: Wallingford, CT, 2009.

12 W. J. Hehre, R. Ditchfield and J. A. Pople, *J. Chem. Phys.* 1972, **56**, 2257.